Sleep and Breathing (2022) 26:1791–1799
https://doi.org/10.1007/s11325-022-02562-w

SLEEP BREATHING PHYSIOLOGY AND DISORDERS • ORIGINAL ARTICLE

The reduced contraction capacity of palatopharyngeal muscle in OSAHS is related to the decreased intra-cellular [Ca^{2+}] mediated by low RyR1 and DHPRα1s expression

Mengmeng Wang[1,2] · Qian Zhao[1] · Zitai Ma[1] · Huaian Yang[2] · Liying Hao[3] · Ke Du[1]

Received: 22 June 2021 / Revised: 31 December 2021 / Accepted: 5 January 2022 / Published online: 13 January 2022

Abstract

Purpose To aim of the study was to explore the possible mechanisms for the decreased contraction capacity of the palatopharyngeal muscle in cases with obstructive sleep apnea hypopnea syndrome (OSAHS).

Methods Palatopharyngeal muscle specimens from patients with OSAHS were taken as the case group. Palatopharyngeal muscle tissue by surgical removal of oropharyngeal malignant tumors was used as a control cohort. The palatopharyngeal muscle contraction capacity was measured by assessing diaphragm peak-twitching force / cross-sectional area (Pt/CSA), fatigue index (FI) twitch tension, and force per cross-sectional area (Force/CSA). Myofibril and sarcoplasmic reticulum (SR) ultra-structures were observed by electron microscopy. The intra-cellular calcium concentration was measured by fluorescence spectrophotometry. DHPRα1s and RyR1 expression profiles were probed through RT-qPCR and Western blot, and the colocalization of them was determined by immunofluorescence.

Results In comparison with the control cohort, the OSAHS cohort demonstrated decreased Pt/CSA ($P<0.01$), FI twitch tension ($P<0.01$), together with contraction capacity ($P<0.01$). This cohort also had lower intra-cellular [Ca^{2+}] of palatopharyngeal muscle cells with abnormal ultrastructure of sarcoplasmic reticulum (SR) ($P<0.01$). In addition, transcriptomic ($P<0.01$) and proteomic expression ($P<0.01$) for RyR1 and DHPRα1s were markedly reduced within OSAHS cohort, although the degree of colocalization of them was not altered.

Conclusion RyR1 and DHPRα1s downregulation may disrupt intra-cellular [Ca^{2+}] homeostasis and subsequently decrease the palatopharyngeal muscle contraction capacity in patients with OSAHS, thus providing a novel insight into the pathogenesis of OSAHS.

Keywords OSAHS · Palatopharyngeal muscle · Intra-cellular calcium concentration · RyR1 · DHPRα1s

Introduction

Obstructive sleep apnea hypopnea syndrome (OSAHS) of varying degrees has been prevalent worldwide as a major public health concern. Its prevalence rate increases according to numerous risk factors, including obesity, increased older population and adverse habits, such as smoking and drinking. Race and gender may be risk factors for OSAHS, but do not contribute to an increased prevalence [1, 2]. OSAHS is described by repeated collapsing events of the upper-respiratory tract during sleep, due to diminished pharyngeal airway structural-support, together with absence of muscle-toning of the upper-respiratory-tract dilators [3, 4]. Uvulopalatopharyngoplasty (UPPP) is the most common surgical treatment for OSAHS [5]. Even though the dysfunction of upper airway dilator muscle is closely related

Mengmeng Wang, Qian Zhao, and Zitai Ma contributed equally to this work.

✉ Liying Hao
lyhao@cmu.edu.cn

✉ Ke Du
kdu@cmu.edu.cn

[1] Department of Pharmacology, School of Pharmacy, China Medical University, No. 77 of Puhe Road, Shenyang North New Area, Shenyang 110122, Liaoning Province, China

[2] Department of Otolaryngology Head and Neck Surgery, Shengjing Hospital of China Medical University, Shenyang 110122, Liaoning, China

[3] Department of Pharmaceutical Toxicology, School of Pharmacy, China Medical University, No. 77 of Puhe Road, Shenyang North New Area, Shenyang 110122, Liaoning Province, China

to the pathogenesis of OSAHS as it causes upper airway obstruction, the underlying mechanism of this dysfunction remains unclear.

Skeletal muscular contractility relies upon excitation–contraction coupling (ECC) triggering. ECC involves intra-cellular Ca^{2+} homeostasis [6, 7]. Intra-cellular Ca^{2+} concentration ($[Ca^{2+}]$) has pivotal parts within skeletal muscular contractility. Lowering $[Ca^{2+}]$ dramatically reduces skeletal muscle force and the rate of force development [8]. Ryanodine receptors (RyR), an intra-cellular Ca^{2+} discharge-channel found atop the sarcoplasmic reticulum (SR), discharges Ca^{2+} present within intra-cellular stockpiles [9]. Three isoforms exist for RyR (RyR1, RyR2 and RyR3), which are found within skeletal / cardiac / smooth muscle and brain, accordingly [10–12]. The dihydropyridine receptor (DHPR), an L-type Ca^{2+} channeling-complex, is spread across the transverse tubule developed through depression over cellular membrane/s. DHPR is segregated within skeletal-(DHPRα1s) / cardiac-muscle (DHPRα1c) isoforms [13, 14]. The calcium-discharging protein for ECC is based upon RyR1 / DHPRα1s, both of which are essential for ECC within skeletal muscle-tissue [15].

In this study, we measured the contraction capacity of palatopharyngeal muscle in OSAHS. To examine the possible mechanistic insight into palatopharyngeal muscle dysfunction, we further explored the intra-cellular $[Ca^{2+}]$ and the expression levels of DHPRα1s and RyR1 and studied their colocalization.

Methods

Clinical Specimen

From April 2020 to February 2021, palatopharyngeal muscle samples were obtained from patients with OSAHS who were treated within the Sleep Medicine Center of Shengjing Hospital, linked with the China Medical University. The patients were diagnosed using polysomnography (AHI 30–50), 3D-CT of upper airway and electronic rhinopharyngoscopy, and modified UPPP was used to treat pharyngeal stenosis. Furthermore, palatopharyngeal muscle samples with oropharyngeal malignant tumors were used as the control cohort (AHI < 5) in this hospital. Palatopharyngeal muscle tissue unadhered to the tumor was obtained by the surgical removal of the tumor from the soft tissue safety margin of 1 cm. The study was reviewed and approved by the Ethics Committee of the China Medical University, and signed informed consent was collected for all the participants.

Isolation of Palatopharyngeal Muscle Cells in Vitro

The palatopharyngeal muscle was washed three times with bicarbonate-based buffering solution and continuously aerated using 95% O_2–5% CO_2 for removing blood contamination. After cleansing the muscle, it was placed in Dulbecco's modified Eagle medium (DMEM) and aerated using 95% O_2 – 5% CO_2 (pH 7.4) at 4 °C to remove non-muscle tissue. The fibers were dissected to produce 2–4 mm-thickness segments, consequently transferred within conical tubes containing DMEM medium augmented with 0.025 mg/mL type I collagenase, 0.025 mg/mL type-II collagenase, together with 2 mg/mL bovine serum albumin (BSA) (10 min at 37 °C). Following three centrifuging steps (500 × *g*—three minutes per step), the supernatant was removed. DMEM solution was introduced and allowed to mix for 3–5 min. Post-centrifugation (800 × *g* for 3–5 min), palatopharyngeal muscle cells having adequate visual features (encompassing cellular membrane integrity, no visible bubbles or particles, decent permeability, and clear-striations) were obtained.

Measurement of Palatopharyngeal Muscle Contractile Function

We measured the palatopharyngeal muscle contractional level in vitro. Isometric contractility together with in-vitro FI were identified within previously published investigations [14]. The palatopharyngeal muscle strips were placed briefly immersed within Krebs–Ringer's solution bath. Individual muscular strips were in-vitro triggered through monophasic-rectangular 1.5 ms, implemented using a current-amplifier (Grass S88; Astro-Med, West Warwick, Rhode Island, USA). Current intensity was regulated until observing the palatopharyngeal muscle maximal tetanic force (P_0; 50 Hz and 500 ms train) reactions could be visualized. The length of the muscle (L_0) producing maximal isometric tension was determined. Upon L_0, the peak-twitch force (P_t) was identified through a serial contraction-events driven through single-pulse stimulus. Palatopharyngeal muscle force–frequency curves (estimated at 10, 20, 40, 50, 75 and 100 Hz) were identified via stimuli of one-second duration trains having minimal inter-stimulus intervals of 120 s. The palatopharyngeal muscle fatigue was evaluated through stimuli at 40 Hz within 330-ms-duration trains, with one train repeated per second. The FI was calculated as the rate of force emerged following 120 s of primary-force stimulus. Forces were normalized through muscle CSA, evaluated through: muscle mass (g)/ [L_0 (cm) × muscular-density (g/cm^3)].

Palatopharyngeal Muscle Structure Evaluations

Electron microscopy (EM) runs were conducted, as described within past protocols [14]. To define the structure of muscle fibril using light microscopy, the palatopharynx segments were processed (including their fixing, dehydrating, polymerizing and slicing). Thereafter, such blocks were re-oriented, with ultra-thin segments (50–70 nm) being sliced in-parallel to muscular-fiber axis. Such segments were contrasted using uranyl acetate / bismuth subnitrate for transmission-electron microscopy (EM). Three small blocks were randomly chosen from eight sections, and from each block, ten micrographs in one ultrathin section were selected by systematic sampling (total thirty micrographs / section). A square-grid was placed upon micrographs through Image-Pro plus 6.0® (Media Cybernetics, Inc.™, USA) to assess volume fraction (V_v) by point counting of normal myofibril (NMF) and normal SR (NSR). V_v for both NMF / NSR were point numbers for individual categories, reflecting percentage of global point-numbers / tissue-section.

Intra-cellular Calcium Concentration Measurement

The palatopharyngeal muscle cells (1×10^6 cells / mL) were briefly treated using Fluo-3-AM (5 µmol / L) within DMEM (37 °C / 30-min) followed by centrifuging ($600 \times g$). After washing with Hank's balanced salt solution, the cells were observed under a fluorescence spectrophotometer (Model F4500®; Hitachi™, Japan) (37 °C). Fluo-3-AM was 488 nm stimulated, with emission recorded at 526 nm. Throughout such assays, cells were exposed to ethylene–glycol tetra-acetic acid (10 mmol / L) and Triton X-100 (0.1%) for obtaining minimum / maximum fluorescence. Dissociation constant for Fluo-3-AM was 400 nmol / L.

Real-time PCR

Palatopharyngeal muscle was homogenized, and the total RNA was isolated. This was reverse transcribed into cDNA through PrimeScript RT® (Takara™, Japan) in line with kit instructions. Consequently, cDNA was amplified through SYBR Premix Ex Taq II® (Takara™, Japan) using a real-time PCR-platform (FTC-3000®, Canada). The cDNA was consequently employed as template within polymerase chain reaction (PCR) runs through a DNA thermal cycler-setup (Perkin-Elmer™, USA).

Western Blot

Such assays were conducted according to previous methods [16]. Membranes were exposed to 1° antibodies for DHPRα1 (1: 1000, Abcam™), RyR1 (1: 1000, Abcam™), and β-actin (1: 1000, SantaCruz™) followed by exposure to second antibodies linked with horseradish-peroxidase (1: 2000; Santa Cruz™). Immuno-reactive bands were identified visually through enhanced chemiluminescent kit (ECL + ®, Amersham Biosciences™) and quantified through Quality One® (BioRad™).

Immunofluorescence (IF)

Prior to staining, specimens were fixated onto slides employing fresh 4% paraformaldehyde (20-min duration) followed by triple-wash steps (five minutes / step) using phosphate-buffered saline (PBS) solution (pH 7.4). To compare the distribution of DHPRα1 and RyR1, double labeling experiments were performed with DHPRα1 (1: 500; Abcam™) monoclonal-antibody together with RyR1 (1: 500; Abcam™) monoclonal-antibody. First, segments were placed into incubation within PBS augmented through 1% bovine BSA for blocking nonspecific binding-sites, and consequently placed into incubation with DHPRα1 (1: 1,000; Abcam™) / RyR1 antibodies (1: 1,000; Abcam™) overnight (4 °C). Consequently, segments were treated to three PBS/BSA washing-steps (ten-minute duration / step) with a subsequent 1-h incubating timeframe with the relevant second antibody (1: 2,000; Abcam™) conjugated to fluorescein isothiocyanate. This 2° antibody triple-rinsed using PBS. Regarding stain-patterns to not rely on the sequence in which the tissue was exposed to the different primary antibodies, primary antibodies were applied in reverse order during the premier double staining experiments. Final steps involved samples being scrutinized using inverted laser-confocal scanning-microscopy (Nikon™ Digital Eclipse C1®, Japan). Such images were gathered, digitized and assessed through Image-Pro Plus 6.0® (Media Cybernetics, Inc.™).

Statistical Analyses

Dataset outcomes reflected mean ± standard deviation. T-test was employed for comparative analyses of both cohorts through SPSS® (version 19.0; SPSS Inc.™, USA). Any variations across both cohorts was deemed to confer statistical significance at $P < 0.05$.

Results

Palatopharyngeal Muscle Contractile Function

When examining the contraction capacity of the palatopharyngeal muscle, Pt (5.27 ± 0.52 N/cm^2 within the control cohort; 3.24 ± 0.36 N/cm^2 within the OSAHS cohort) and FI (62.1 ± 3.5% within the control cohort; 45.2 ± 1.9% within the OSAHS cohort) were found to be markedly reduced in the 50 OSAHS samples in

comparison with those within the 15 control samples (Fig. 1a and b). In addition, the contraction capacity in the OSAHS cohort was remarkably reduced throughout the implemented triggering frequency-range (Fig. 1c). These results demonstrated the abnormal contractile function of palatopharyngeal muscle in patients with OSAHS.

Intra-cellular [Ca^{2+}] of Palatopharyngeal Muscle Cells

Intra-cellular [Ca^{2+}] is closely related to skeletal muscle contraction. Measurement of the intra-cellular [Ca^{2+}] of palatopharyngeal muscle cells demonstrated that the intra-cellular [Ca^{2+}] within the OSAHS cohort (680.7 ± 13.9 nM) was markedly lower than that within control cohort (968.5 ± 18.8 nM) (Fig. 2). This indicated that the dysfunction of palatopharyngeal muscle contraction capacity was relative to the disruption of intra-cellular Ca^{2+} homeostasis.

Ultrastructure of the Myofibril and SR

SR is the main intra-cellular Ca^{2+} stockpiling and discharging organelle within muscular cells. The SR and myofibril ultrastructures in palatopharyngeal muscle were examined using EM. The SR demonstrated an abnormal state in the OSAHS cohort in comparison with the control cohort (as marked by the arrow, Fig. 3a). Myofibril destruction was not observed in the OSAHS cohort (Fig. 3a). Furthermore, the V_v for NSR was remarkedly reduced in the OSAHS cohort (7.4 ± 1.4%) in comparison with that in the control cohort (13.7 ± 1.0%), but the V_v of NMF in the OSAHS cohort (85.3 ± 7.1%) demonstrated no significant difference from that in the control cohort (86.1 ± 7.2%) (Fig. 3b).

Expression Levels and Colocalization of RyR1 and DHPRα1s

Ca^{2+} release from the SR during skeletal muscle contraction is mediated by RyR1 and DHPRα1s. The expression-profiles

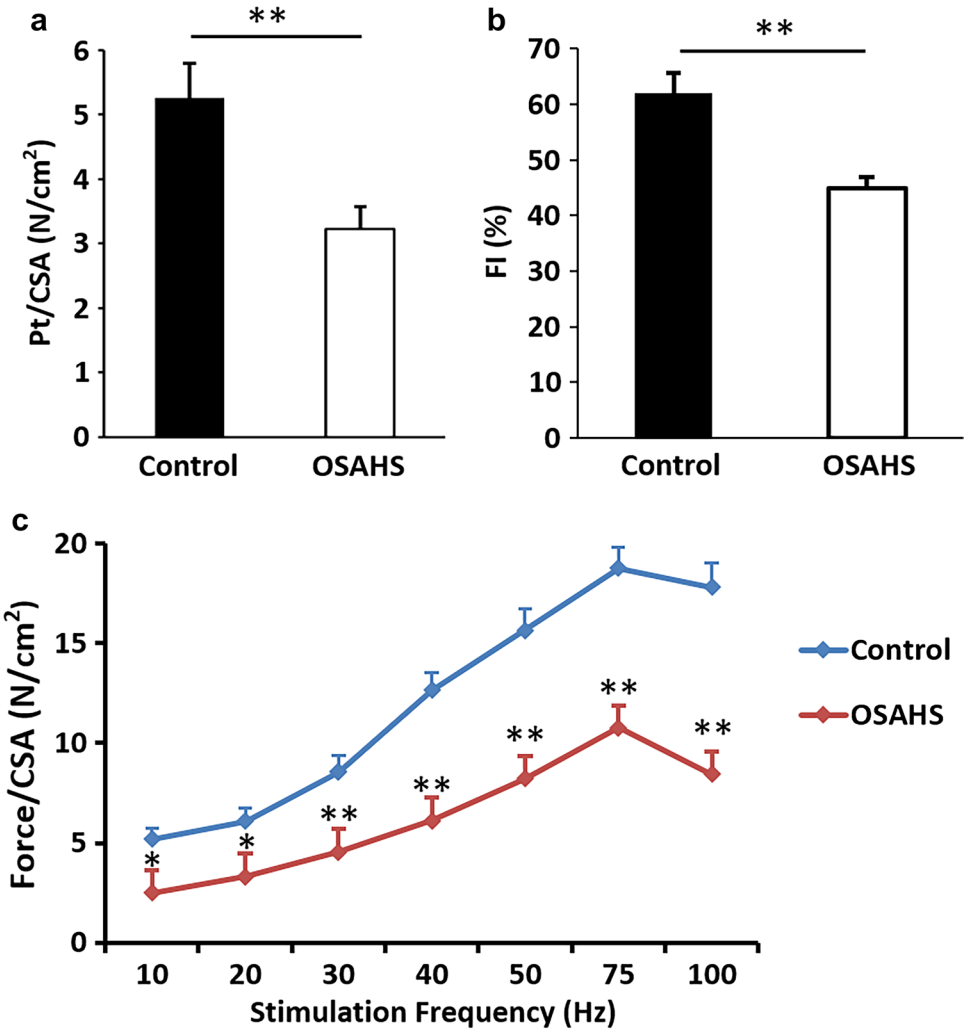

Fig. 1 Palatopharyngeal muscle contraction capacity. **(a)** Peak twitching-force (Pt/CSA) was markedly reduced in the OSAHS cohort in comparison with the control cohort. **(b)** Fatigue index (FI) was markedly reduced in the OSAHS cohort in comparison with the control cohort. **(c)** Palatopharyngeal muscle contraction capacity in the OSAHS cohort was less intense throughout implemented stimulatory frequencies (10–100 Hz) in comparison with controls. $^{*}P < 0.05$, $^{**}P < 0.01$ against control

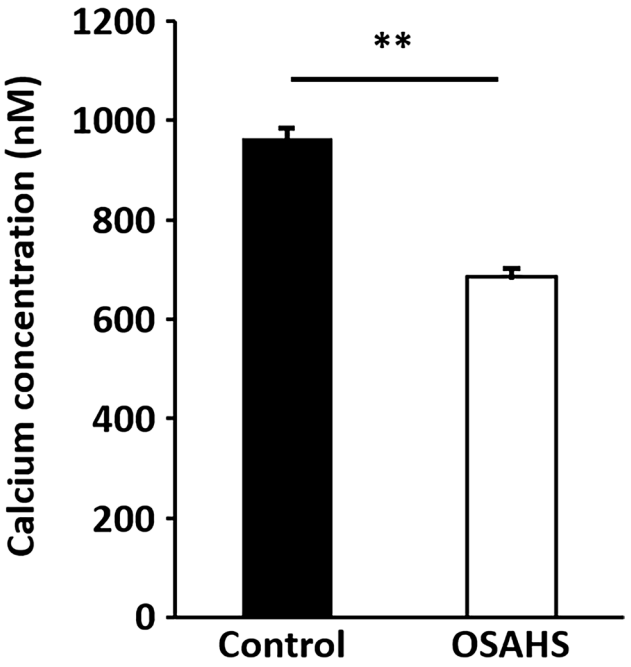

Fig. 2 Intra-cellular calcium within palatopharyngeal muscle cells determined through fluorescence spectrophotometry. Intra-cellular [Ca^{2+}] was markedly reduced within OSAHS cohort in comparison with the control cohort. $^{**}P < 0.01$ against control

/ colocalization for RyR1 / DHPRα1s in OSAHS samples were measured. Both transcriptomic (Fig. 4a and b) / proteomic profiles (Figs. 4c-e, 5a and b) for RyR1 / DHPRα1s in the OSAHS cohort were markedly reduced. Notwithstanding, Mander's overlap coefficients demonstrated that the colocalization for both molecular players was not significantly shifted in the OSAHS cohort (Fig. 5a and c). These results suggested that Ca^{2+} homeostasis imbalance in patients with OSAHS was associated with DHPRα1s / RyR1 downregulation.

Discussion

Although it is well known that the dysfunction of upper airway dilator muscle is closely associated with the pathogenesis of OSAHS, the mechanism underlying this dysfunction has rarely been reported. Here, we found that upper airway dilator muscle dysfunction was associated with intra-cellular [Ca^{2+}] imbalance and abnormal expression of RyR1 and DHPRα1 in patients with OSAHS, and provided further mechanistic insight into the upper airway muscle dysfunction in OSAHS.

As sleep occurs, the resistance of the pharyngeal airway changes from low to high. There is an increase in upper airway resistance when patients with OSAHS wake up [17]. Observation of patients with OSAHS suggests that as the state of waking turns to sleep, the diameter of the pharyngeal airway will change rapidly and reversibly, and the muscle strength of one or more parts of the pharyngeal airway decreases [18]. The palatopharyngeal muscle is the main dilatation muscle within the upper airway, and its abnormal functioning can directly lead to the loss of airway patency [19]. This muscle is closely related to the pathogenesis of OSAHS [20]. The palatopharyngeal muscle injury in OSAHS is associated with an efferent neuropathy [21], even though the evidence of muscle denervation affecting the upper airway dilator muscles is lacking [22]. Boyd and colleagues suggested that inflammatory cell infiltration affects the palatopharyngeal muscle of patients with OSAHS [20]. Recently, *Dong* et al. reported that the pathogenesis of OSAHS appeared to involve pharyngeal muscle cell apoptosis via mitochondrial-mediated apoptotic pathway [19]. Consistent with the results of previous studies, in this study, we also observed the malfunctioning of the palatopharyngeal muscle with reduced contraction capacity in the OSAHS cohort. This dysfunction was associated with [Ca^{2+}] homeostasis imbalance and downregulated DHPRα1s / RyR1. [Ca^{2+}] homeostasis within skeletal muscle-tissue is mainly regulated by RyR1 and DHPRα1s expression-profiles and the physical interaction between them [14, 15]. The RyR1-I4898T mutation, which is expressed on the skeletal muscle SR, results in exacerbated RyR1 function and intra-cellular [Ca^{2+}] leaks [23]. RyR1-related myopathies and mutations in dyspedic myotubes lead to a reduction in voltage-gated Ca^{2+} release and uncouple EC-coupling [24], and congenital myopathies, such as Duchenne muscular dystrophy and Limb–Girdle muscular dystrophy were reported as associated with RyR1 issues / altered Ca^{2+} homeostasis [25, 26]. Skeletal DHPRα1s directly interact with RyR1 leading to Ca^{2+} release from SR, triggering ECC within skeletal muscle [27]. Ca^{2+} transient release is strongly affected by mutations in RyR1 that diminishes its binding to DHPR [28]. Weakened diaphragmatic contraction capacity within septic rats has been linked to down-regulated DHPRα1s / RyR1 [15]. The above dataset outcomes support our findings regarding dysfunction of pharyngeal muscle in patients with OSAHS that may correlate with the decreased intra-cellular [Ca^{2+}] mediated by RyR1 / DHPRα1s dysregulations. Furthermore, EM results exhibited pathological ultrastructures of SR in the OSAHS cohort. Thus, it is speculated that the altered SR is one of the causes for the DHPRα1s / RyR1 dysfunction in SR, leading to impaired ECC execution and decreased muscular contraction capacity. Further investigations will be required to precisely elucidate the mechanisms involved in these processes.

In recent years, researchers have focused on the development of alternative treatment strategies targeting upper airway dilator muscles muscle activation, including non-pharmacological and pharmacological interventions. Regarding

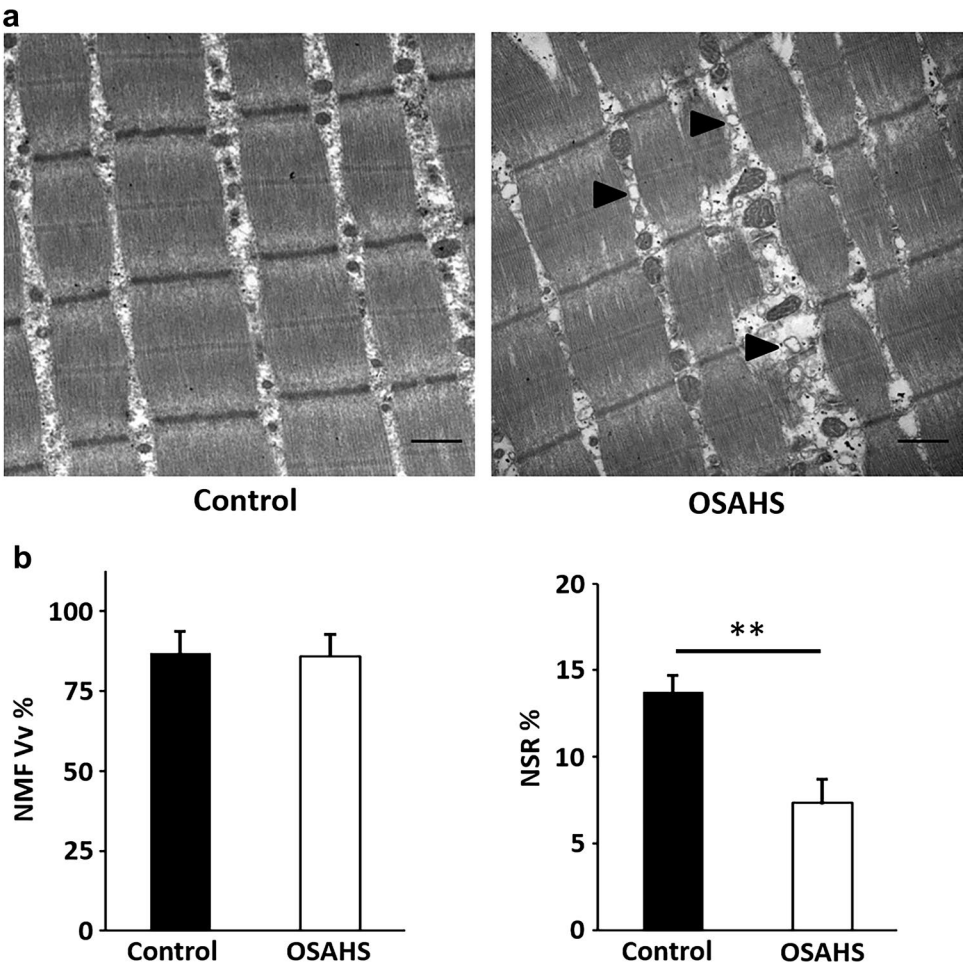

Fig. 3 Myofibril and SER detailed structures. **(a)** Electron microscopy revealed NMF / NSR ultra-structure. The SR was modified (abnormal SR, arrowheads), through myofibril remained unmodified in OSAHS muscle. Scale = 1 μm. **(b)** V_v for NMF remained unmodified in the OSAHS cohort in comparison with the control cohort. V_v for NSR was markedly reduced in the OSAHS cohort in comparison with controls. Values existed < 100%, since V_v for other cellular organelles (e.g., mitochondria, interstitium and nuclei) were excluded. $^{**}P < 0.01$ against control

OSA pharmacotherapy, AAV9-DREADD may trigger the genioglossus muscle, improving pharyngeal patency and breathing effectiveness throughout sleep in a mouse model of OSAHS [29]. Selective norepinephrine reuptake inhibitors can mitigate OSA in most patients by increasing the activity of pharyngeal dilator muscles [30]. Regarding OSA non-pharmacological interventions, hypoglossal nerve stimulation is used to increase upper airway muscle phasic activity during sleep [30]. However, the mechanism of these drugs or medical treatments for OSA remains unclear. In particular, whether or not it is related to palatopharyngeal muscle function via regulating intra-cellular $[Ca^{2+}]$ and the expression of RyR1 and DHPRα1 remains to be further studied. In addition, based on our findings, we cautiously suggest that new medical research targeting RyR1 and DHPRα1 that improves palatopharyngeal muscle function may provide effective treatment for OSA.

There are limitations to our study. It is better to use palatopharyngeal muscle tissue from healthy volunteers as a control cohort rather than from patients with oropharyngeal malignant tumors. However, it was not possible for us to obtain palatopharyngeal muscle tissue from healthy volunteers clinically. As an alternative, we have obtained the palatopharyngeal muscle tissue unadhered to the tumor by the surgical removal of the tumor from the soft tissue within safety margins. We also assessed the palatopharyngeal muscles using microscopy to make sure that it contained no tumor tissue.

With present study, we identified low intra-cellular $[Ca^{2+}]$, weakness of pharyngeal muscle contraction capacity, altered SR, and reduced expression of RyR1 and DHPRα1s in OSAHS. We surmise that the abnormal function of RyR1 and DHPRα1s within SR may result in decreased intra-cellular $[Ca^{2+}]$ release, challenged ECC execution, together with pharyngeal muscle issues in OSAHS.

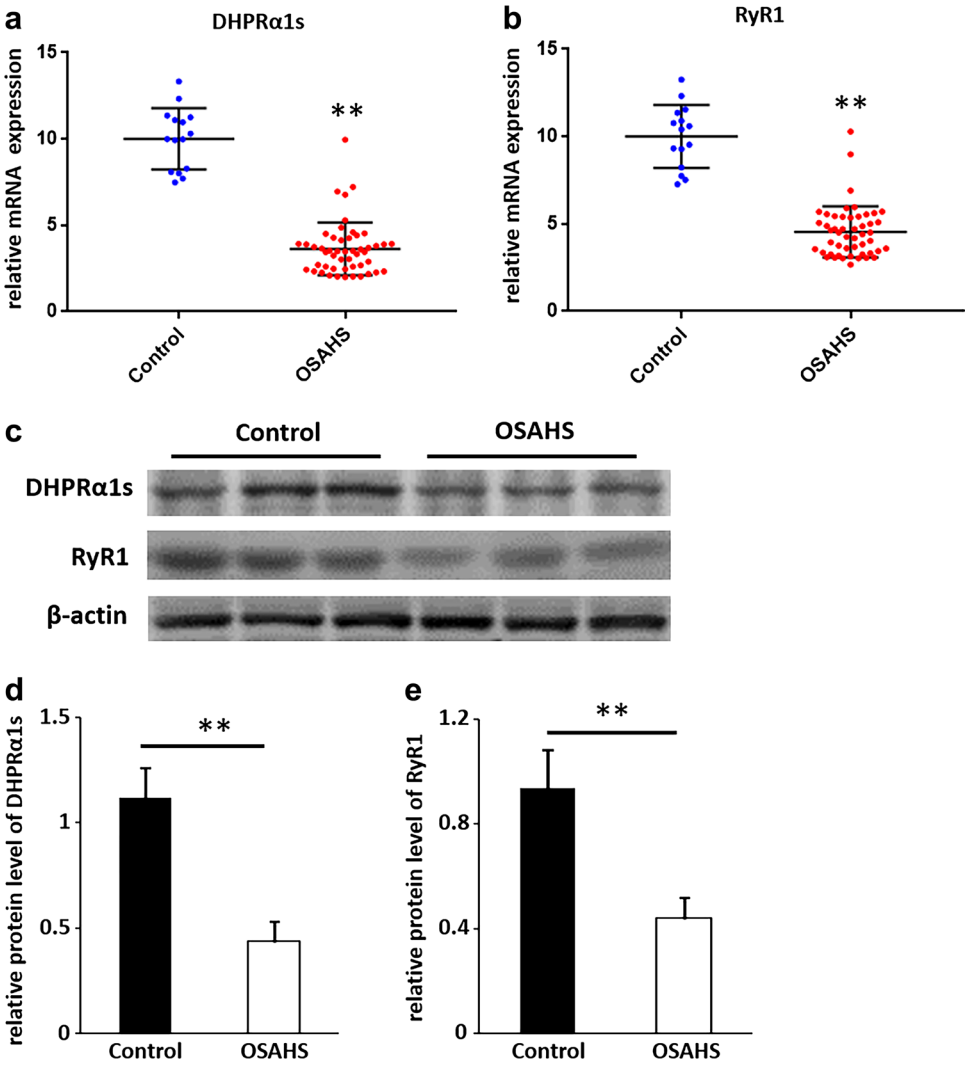

Fig. 4 RyR1 / DHPRα1s transcriptomic expression profiling. **(a and b)** The results of real-time PCR demonstrated the mRNA expression for RyR1 / DHPRα1s in the OSAHS cohort to be downregulated in comparison with the control cohort. **(c-e)** RyR1 / DHPRα1s proteomic level profiling was evaluated through Western blotting. Relative proteomic expression for RyR1 / DHPRα1s was normalized against β-actin. $^{**}P < 0.01$ against control

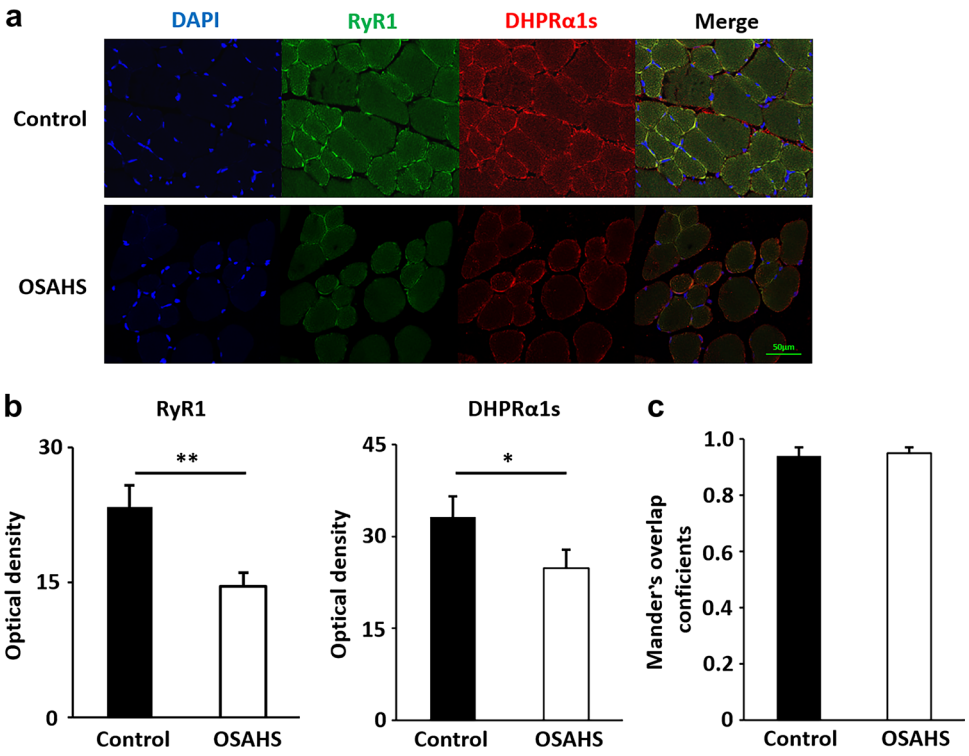

Fig. 5 Colocalization / expression-profiling for RyR1 / DHPRα1s through immunofluorescence. **(a)** Immunofluorescence-based distribution of RyR1 (green) and DHPRα1s (red). RyR1 colocalized with DHPRα1s (merge). Scale bar = 50 μm. **(b)** Immunofluorescence highlighted reduced optical densities for RyR1 / DHPRα1s in the OSAHS cohort in comparison with the control cohort. **(c)** Mander's overlap coefficients indicated co-localization for RyR1 / DHPRα1s as unmodified in the OSAHS cohort in comparison with the control cohort. $^{*}P < 0.05$, $^{**}P < 0.01$ against control

Abbreviations BSA: Bovine serum albumin; CSA: Cross-sectional area; DHPRa1s: Dihydropyridine receptors; DMEM: Dulbecco's modified Eagle medium; ECC: Excitation–contraction coupling; EM: Electron microscopy; FI: Fatigue index; IF: Immunofluorescence; L_0: Length of the muscle produced maximal isometric tension; NMF: Normal myofibril; NSR: Normal sarcoplasmic reticulum; OSAHS: Obstructive sleep apnea hypopnea syndrome; P_0: Maximal tetanic force; PBS: Phosphate-buffered saline; Pt: Peak twitch force; RyR1: Ryanodine receptor; SER: Smooth endoplasmic reticulum; SR: Sarcoplasmic reticulum; V_v: Volume fraction

Authors' contributions KD, LH and MW conceived and designed the experiments. MW, QZ, ZT M and HY performed the examination and prepared Figures. KD and LH wrote the manuscript; KD, LH and MW reviewed the manuscript. All authors read and approved the final manuscript.

Funding This study was supported by Youth backbone support Program of China Medical University (QGJ2018061).

Availability of data and material The datasets used and/or analyzed during the current study are available from the corresponding author on reasonable request.

Code availability Not applicable.

Declarations

Conflicts of interest None of the authors has any conflict of interest to disclose.

Ethics approval and consent to participate Ethical approval was obtained from the ethics committee of Shengjing Hospital of China Medical University (2020PS363K(X1)) and informed consent obtained from all participants.

Consent for publication Not applicable.

References

1. Lee JJ, Sundar KM (2021) Evaluation and Management of Adults with Obstructive Sleep Apnea Syndrome. Lung 199(2):87–101
2. Mohit A, Shrivastava P (2021) Chand, Molecular determinants of obstructive sleep apnea. Sleep Med 80:105–112
3. Ko CY, Liu QQ, Su HZ, Zhang HP, Fan JM, Yang JH, Hu AK, Liu YQ, Chou D, Zeng YM (2019) Gut microbiota in obstructive sleep apnea-hypopnea syndrome: disease-related dysbiosis and metabolic comorbidities. Clin Sci (Lond) 133(7):905–917
4. Garg RK, Afifi AM, Sanchez R, King TW (2016) Obstructive Sleep Apnea in Adults: The Role of Upper Airway and Facial Skeletal Surgery. Plast Reconstr Surg 138(4):889–898
5. Zhan X, Li L, Wu C, Chitguppi C, Huntley C, Fang F, Wei Y (2019) Effect of uvulopalatopharyngoplasty (UPPP) on atherosclerosis and cardiac functioning in obstructive sleep apnea patients. Acta Otolaryngol 139(9):793–797
6. Eshima H, Poole DC, Kano Y (2014) In vivo calcium regulation in diabetic skeletal muscle. Cell Calcium 56(5):381–389
7. Allen DG, Lamb GD, Westerblad H (2008) Impaired calcium release during fatigue. J Appl Physiol (1985) 104(1):296–305
8. Luo Y, Rall JA (2006) Regulation of contraction kinetics in skinned skeletal muscle fibers by calcium and troponin C. Arch Biochem Biophys 456(2):119–126

9. Kushnir A, Wajsberg B, Marks AR (2018) Ryanodine receptor dysfunction in human disorders. Biochim Biophys Acta Mol Cell Res 1865(11 Pt B):1687–1697
10. Clancy JS, Takeshima H, Hamilton SL, Reid MB (1999) Contractile function is unaltered in diaphragm from mice lacking calcium release channel isoform 3. Am J Physiol 277(4 Pt 2):R1205–R1209
11. Fill M, Copello JA (2002) Ryanodine receptor calcium release channels. Physiol Rev 82(4):893–922
12. Ogawa Y, Kurebayashi N, Murayama T (2000) Putative roles of type 3 ryanodine receptor isoforms (RyR3). Trends Cardiovasc Med 10(2):65–70
13. Dulhunty AF, Wei-LaPierre L, Casarotto MG, Beard NA (2017) Core skeletal muscle ryanodine receptor calcium release complex. Clin Exp Pharmacol Physiol 44(1):3–12
14. Wang MM, Hao LY, Guo F, Zhong B, Zhong XM, Yuan J, Hao YF, Zhao S, Sun XF, Lei M, Jiao GY (2017) Decreased intracellular [Ca(2+)] coincides with reduced expression of Dhpralpha1s, RyR1, and diaphragmatic dysfunction in a rat model of sepsis. Muscle Nerve 56(6):1128–1136
15. Jiao GY, Hao LY, Gao CE, Chen L, Sun XF, Yang HL, Li Y, Dai YN (2013) Reduced DHPRalpha1S and RyR1 expression levels are associated with diaphragm contractile dysfunction during sepsis. Muscle Nerve 48(5):745–751
16. Du K, Liu M, Zhong X, Yao W, Xiao Q, Wen Q, Yang B, Wei M (2018) Epigallocatechin Gallate Reduces Amyloid beta-Induced Neurotoxicity via Inhibiting Endoplasmic Reticulum Stress-Mediated Apoptosis. Mol Nutr Food Res 62(8):e1700890
17. Tangel DJ, Mezzanotte WS, White DP (1991) Influence of sleep on tensor palatini EMG and upper airway resistance in normal men. J Appl Physiol (1985) 70(6):2574–81
18. Malhotra A, Fogel RB, Edwards JK, Shea SA, White DP (2000) Local mechanisms drive genioglossus activation in obstructive sleep apnea. Am J Respir Crit Care Med 161(5):1746–1749
19. Dong J, Niu X, Chen X (2020) Injury and Apoptosis in the Palatopharyngeal Muscle in Patients with Obstructive Sleep Apnea-Hypopnea Syndrome. Med Sci Monit 26:e919501
20. Boyd JH, Petrof BJ, Hamid Q, Fraser R, Kimoff RJ (2004) Upper airway muscle inflammation and denervation changes in obstructive sleep apnea. Am J Respir Crit Care Med 170(5):541–546
21. Friberg D, Ansved T, Borg K, Carlsson-Nordlander B, Larsson H, Svanborg E (1998) Histological indications of a progressive snorers disease in an upper airway muscle. Am J Respir Crit Care Med 157(2):586–593
22. Series F, Simoneau JA, St Pierre S (2000) Muscle fiber area distribution of musculus uvulae in obstructive sleep apnea and non-apneic snorers. Int J Obes Relat Metab Disord 24(4):410–5
23. Lynch PJ, Tong J, Lehane M, Mallet A, Giblin L, Heffron JJ, Vaughan P, Zafra G, MacLennan DH, McCarthy TV (1999) A mutation in the transmembrane/luminal domain of the ryanodine receptor is associated with abnormal Ca2+ release channel function and severe central core disease. Proc Natl Acad Sci U S A 96(7):4164–4169
24. Avila G, Dirksen RT (2001) Functional effects of central core disease mutations in the cytoplasmic region of the skeletal muscle ryanodine receptor. J Gen Physiol 118(3):277–290
25. Andersson DC, Meli AC, Reiken S, Betzenhauser MJ, Umanskaya A, Shiomi T, D'Armiento J, Marks AR (2012) Leaky ryanodine receptors in beta-sarcoglycan deficient mice: a potential common defect in muscular dystrophy. Skelet Muscle 2(1):9
26. Bellinger AM, Reiken S, Carlson C, Mongillo M, Liu X, Rothman L, Matecki S, Lacampagne A, Marks AR (2009) Hypernitrosylated ryanodine receptor calcium release channels are leaky in dystrophic muscle. Nat Med 15(3):325–330
27. Samso M (2015) 3D Structure of the Dihydropyridine Receptor of Skeletal Muscle. Eur J Transl Myol 25(1):4840
28. Cheng W, Altafaj X, Ronjat M, Coronado R (2005) Interaction between the dihydropyridine receptor Ca2+ channel beta-subunit and ryanodine receptor type 1 strengthens excitation-contraction coupling. Proc Natl Acad Sci U S A 102(52):19225–19230
29. FleuryCurado T, Pho H, Freire C, Amorim MR, Bonaventura J, Kim LJ, Lee R, Cabassa ME, Streeter SR, Branco LG, Sennes LU, Fishbein K, Spencer RG, Schwartz AR, Brennick MJ, Michaelides M, Fuller DD, Polotsky VY (2021) Designer Receptors Exclusively Activated by Designer Drugs Approach to Treatment of Sleep-disordered Breathing. Am J Respir Crit Care Med 203(1):102–110
30. Perger E, Taranto-Montemurro L (2021) Upper airway muscles: influence on obstructive sleep apnoea pathophysiology and pharmacological and technical treatment options. Curr Opin Pulm Med 27(6):505–513